

Self-supervised Modal and View Invariant Feature Learning

Longlong Jing¹ Yucheng Chen² Ling Zhang¹ Mingyi He² Yingli Tian^{1*}
¹The City University of New York, ²Northwestern Polytechnical University

Abstract

Most of the existing self-supervised feature learning methods for 3D data either learn 3D features from point cloud data or from multi-view images. By exploring the inherent multi-modality attributes of 3D objects, in this paper, we propose to jointly learn modal-invariant and view-invariant features from different modalities including image, point cloud, and mesh with heterogeneous networks for 3D data. In order to learn modal- and view-invariant features, we propose two types of constraints: cross-modal invariance constraint and cross-view invariance constraint. Cross-modal invariance constraint forces the network to maximum the agreement of features from different modalities for same objects, while the cross-view invariance constraint forces the network to maximum agreement of features from different views of images for same objects. The quality of learned features has been tested on different downstream tasks with three modalities of data including point cloud, multi-view images, and mesh. Furthermore, the invariance cross different modalities and views are evaluated with the cross-modal retrieval task. Extensive evaluation results demonstrate that the learned features are robust and have strong generalizability across different tasks.

1. Introduction

Self-supervised feature learning methods learn visual features from large-scale datasets without requiring any manual annotations. The core of the self-supervised feature learning is to define a pretext task and the visual features are learned through the processing of accomplishing the pretext task. Since it can be easily scaled up to large-datasets, recently some self-supervised methods achieved comparable or even better performance on some downstream tasks than supervised learning methods [30, 17, 7, 2, 24].

Most of the existing self-supervised feature learning methods only focus on learning features for one modality. As a rising trend to model 3D visual features, various methods were proposed to learn point cloud features from point cloud either by reconstructing point cloud [1, 10, 54, 57],

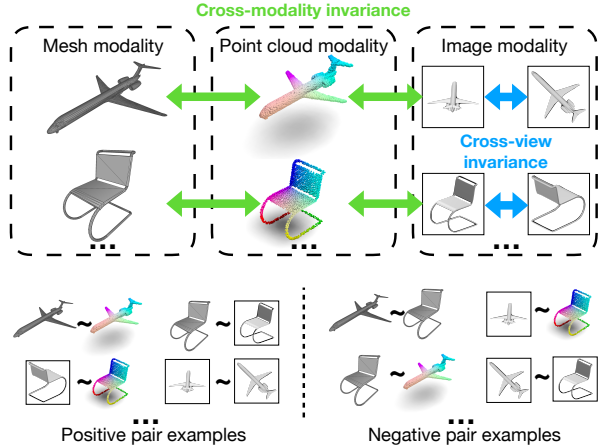


Figure 1. Multi-modality and multi-view representations of 3D objects and pair examples. With cross-modal invariance and cross-view invariance constraints, modal- and view-invariant features can be obtained with heterogeneous networks for different modalities and views of data.

by generating point cloud with Generative Adversarial Networks [29, 46, 51], or by accomplishing pretext tasks [16, 55]. Only a few of them [22] explored to use cross-modality correspondence of 3D data as supervision signal for 3D self-supervised feature learning.

Generally 3D data are inherently multi-modalities. Fig. 1 shows different modalities of same objects in mesh, point cloud, and multi-view images. No matter what data format is used to represent an object, its identity remains unchanged. Thus, it is possible to learn features for an object that invariant to its modalities and views. A straightforward idea is to employ the identity invariance of different modalities and views as supervision signals to learn features from unlabeled data. Jing *et al.* [22] formulated the identity invariance as a classification task and jointly trained multiple networks to verify whether the inputs from different modalities belong to same object by using the cross-entropy loss. However, the learned features, are not modality-invariant which make it impossible to directly compare the features from different modalities of 3D data.

Recently, contrastive learning has shown great promise and obtained promising performance for recent self-

*Corresponding author. Email: ytian@ccny.cuny.edu

supervised feature learning methods [7, 17, 14]. Similar to triplet loss [41], contrastive loss is to maximize the feature similarity between positive pairs and minimize the feature similarity of other negative pairs. The most commonly used approach to generate positive and negative training pairs is data augmentation on input data [3, 7, 17]. However, dramatic data augmentation, such as cutout and jittering, inevitably changes the distribution of the training inputs far from the real testing data.

To enable heterogeneous networks to learn features of different modalities and views in same universal space, in this paper, we propose to employ two constraints derived from the attributes of 3D data as supervision signal for self-supervised learning: cross-modal invariance constraint and cross-view modal invariance constraint. The cross-modal invariance constraint forces networks to learn identity features from different modalities of the same object, while the cross-view invariance constraint forces networks to learn an identity features for each object regardless of its view. When jointly learned with the two constraints, modal- and view-invariant features in the universal space can be obtained for each object.

Inspired by the contrastive learning [7], we propose a framework to capture modal-invariant and view-invariant features with heterogeneous networks on three different modalities including mesh, point cloud, and multi-view images. Specifically, the features from different modalities and rendered views of 3D objects are extracted with corresponding subnetworks and combined as positive pairs (sampled with the same object identity) and negative pairs (sampled with different object identities). Then the feature distance of positive cross-modality pairs is minimized, and the feature distance of negative cross-modality pairs is maximized by using contrastive loss. The modal- and view-invariant features are obtained after optimizing networks with the two types of constraints over the positive and negative pairs. The main contributions of this paper are summarized as follows:

- We propose a novel self-supervised feature learning schema to jointly learn modal- and view-invariant features for 3D objects end-to-end without using any manual labels.
- The proposed framework maps the features of different modalities and views of 3D data into same universal space which makes cross-modal retrieval possible for 3D objects.
- To the best of our knowledge, we are the first to explore the cross-modal retrieval for 3D objects with multiple modalities in a self-supervised learning way..
- The effectiveness and generalization of the learned features are demonstrated with extensive experiments

with three different modalities on five different tasks including 3D object recognition, few-shot 3D object recognition, part segmentation, in-domain 3D object retrieval, and cross-modal retrieval.

2. Related Work

2D Self-supervised Feature Learning: Many methods have been proposed to learn visual features from unlabeled 2D data including videos and images. Based on the source of supervision signal, there are four types of self-supervised learning methods: Generation-based method, context-based method, free semantic label-based method, and cross-modal based method. The generation-based methods learn features by reconstructing the data including Auto-encoder, and Generative adversarial networks [13], super resolution [28], colorization [56], and video future prediction [44]. The context-based methods learn features by using spatial context or temporal context including Jigsaw puzzle [32], geometric transformation [11, 23], clustering [4], frame order reasoning [31]. The free semantic label-based methods learn features either by data from game engine or to distill features from other unsupervised learning features [34]. The cross-modal-based methods learn features by the correspondence between a pair of channels of data including video-audio [27] and video-text. Recently, more researchers explore to apply these self-supervised learning methods to 3D data [22, 55, 40, 16].

3D Self-supervised Feature Learning: Several self-supervised learning methods have been proposed to learn 3D features for point cloud objects by reconstructing point cloud data [1, 10, 54, 57], by generating point cloud with GANs [29, 46, 47, 51], or by training networks to solve pre-defined pretext tasks [16, 40, 55, 22]. Sauder *et al.* proposed to learn point cloud features by training networks to recognize the relative position of two segments of point cloud [40]. Zhang *et al.* designed a clustering followed by contrastive as pretext task to train networks to learn point cloud features. Hassani *et al.* proposed to train networks with multiple pre-defined pretext tasks including clustering, prediction, and reconstruction for point cloud data [16]. Jing *et al.* proposed to utilize cross-modality relations of point clouds and multi-view images as supervision signal to jointly learn point cloud and image features for 3D objects. However, the point cloud and image features by the network in [22] are not modality invariant. To thoroughly utilize the cross-modality inherent attributes of 3D data, here we propose to learn modal- and view-invariant features for 3D objects with three different modalities including point cloud, mesh, and images.

Contrastive Self-supervised Learning: The basic principle of contrastive learning, such as Noise Contrastive Estimation (NCE) [15], is to learn representations by contrasting positive and negative pairs. By maximizing the

similarity between an anchor sample and a positive sample while minimizing similarity to all other (negative) samples, contrastive learning has shown empirical success in self-supervised learning methods [3, 7, 17, 19, 20, 30, 48, 53, 14, 35] of which the core is to generate positive and negative training pairs by pretext tasks. Most recent work performed training pairs generation in image domain. Studies [3, 7, 17] applied dramatic data augmentation such as color jittering, cropping, cutout, and flipping on original images. PIRL [30] cropped an image into jigsaw patches, then combines the original image and the shuffled patches into a positive pair. [19] divided an image into a grid of overlapping patches and predicts the unseen regions by context patches with Contrastive Predictive Coding (CPC) [33]. [14] extended the contrastive learning on videos by sampling frames from same video as multiple positive pairs. Contrastive Multiview Coding (CMC) [48] used transferred representations (such as Lab color space, depth, and segmentation) of a source image as paired samples. Very few work adopted cross-modality invariance on contrastive learning. [35] generated training pairs by video clips and their corresponding audios. The number of negative pairs affects the probability that positive sample paired with hard negative. Some work [30, 53, 14] introduced memory banks storing previous feature outputs to enlarge the negative pairs pool. Momentum Contrast (MoCo) [17] further increased the number of negative samples by a slowly updated negative feature extractor. In this paper, we propose to pair positive and negative object samples by cross-modality invariance in three domains (mesh, point cloud, and image) and cross-view invariance in image domain.

3. Method

An overview of the proposed framework is shown in Fig. 2. The core of our method is to optimize heterogeneous networks to learn modal- and view-invariant features under cross-modality invariance constraint and cross-view invariance constraint by contrasting. Three heterogeneous networks are employed to extract features for three modalities of data including mesh, point cloud, and images, respectively. The framework contains three backbone networks (an image-extracting network F_{img} , a point cloud-extracting graph network F_p , and a mesh-extracting network F_m) and three corresponding projection heads ($F_{img,h}$, $F_{p,h}$, $F_{m,h}$) mapping features of different modalities into the universal space. Two types of constraints including modality-invariant constraint and view-invariant constraint are used to optimize the network by contrasting paired features of all objects in the universal space. The detailed formulation of our approach is explained in subsection 3.1, and the network architectures are described in subsection 3.2.

3.1. Model Parameterization

The contrastive learning enables the networks to learn representations by maximizing the similarity between an anchor sample and a positive sample while minimizing similarity to all other (negative) samples, similar to the triplet loss [41]. In this paper, the positive pairs are sampled from different modality and view representations with same object identity, while negative pairs with different object identities as shown in Fig 1. The contrastive learning implementation in this paper uses the following procedure.

Given a batch of k anchor features $\{A^{(1)}, \dots, A^{(k)}\}$ and k corresponding positive features $\{P^{(1)}, \dots, P^{(k)}\}$. The contrastive loss for this single anchor-positive batch l_{ap} is defined as

$$l_{ap} = -\frac{1}{k} \sum_{i=1}^k \log \frac{e^{sim(A^{(i)}, P^{(i)})}}{\sum_{j=1, j \neq i}^k e^{sim(A^{(i)}, A^{(j)})} + \sum_{j=1}^k e^{sim(A^{(i)}, P^{(j)})}}, \quad (1)$$

where $sim(A, P)$ denotes the pairwise cosine similarity between two feature vectors as shown in Eq. 2. $sim(A^{(i)}, P^{(i)})$ calculates the feature similarity of positive pairs, while all other feature similarity calculations are for negative pairs. The optimization of contrastive loss pulls the positive feature pairs closer and pushes the negative feature pairs further in the universe space.

$$sim(A, P) = A^T P / (\tau \|A\| \|P\|), \quad (2)$$

where τ denotes a temperature parameter. When considering the anchor features as the positive corresponding to original positive features, we can calculate the contrastive loss for the positive-anchor batch l_{pa} as

$$l_{pa} = -\frac{1}{k} \sum_{i=1}^k \log \frac{e^{sim(P^{(i)}, A^{(i)})}}{\sum_{j=1, j \neq i}^k e^{sim(P^{(i)}, P^{(j)})} + \sum_{j=1}^k e^{sim(P^{(i)}, A^{(j)})}}. \quad (3)$$

Therefore, the complete contrastive loss for the anchor-positive combination is

$$L_{AP} = l_{ap} + l_{pa}. \quad (4)$$

Let $\mathcal{D} = \{X^{(1)}, \dots, X^{(N)}\}$ denotes training data with N specific objects. The i -th input sample $X^{(i)} = \{p^{(i)}, m^{(i)}, img_1^{(i)}, img_2^{(i)}\}$, where $m^{(i)}$ and $p^{(i)}$ represent the 3D mesh object and the corresponding sampled point cloud, $img_1^{(i)}$ and $img_2^{(i)}$ are two images under different views generated from the same 3D mesh object. Passing $X^{(i)}$ through the framework, we can obtain corresponding features: $f_p^{(i)}$, $f_m^{(i)}$, $f_{i1}^{(i)}$, and $f_{i2}^{(i)}$. Given a training minibatch $\{X^{(i)}\}_{i=1}^k$ of k samples, the positive pairs are derived from same $X^{(i)}$, while the negative pairs are sampled between $X^{(i)}$ and all other samples. In our

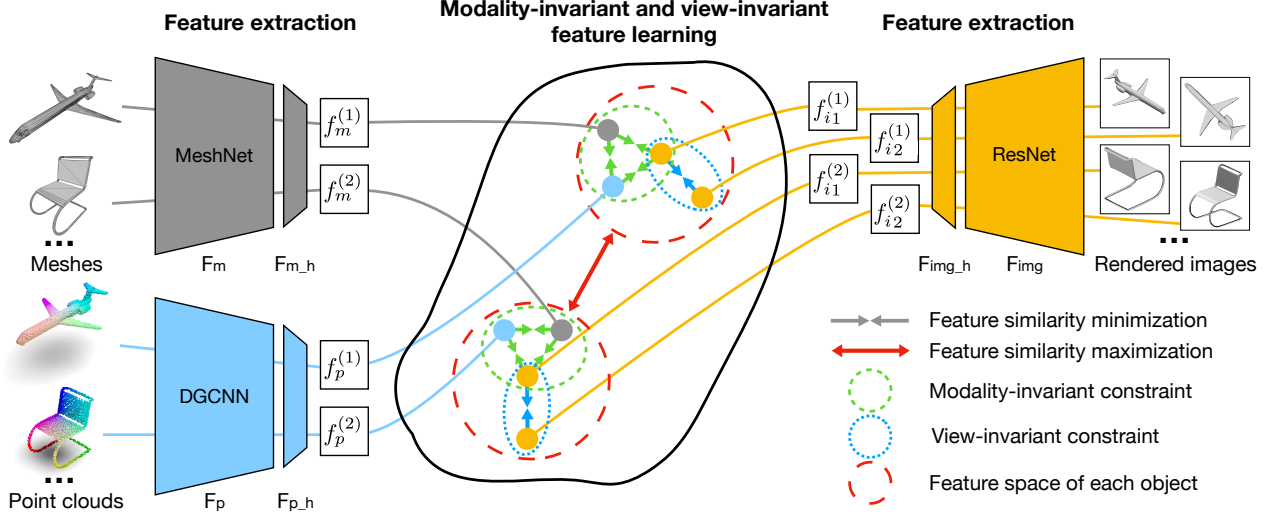


Figure 2. An overview of the proposed self-supervised modal- and view-invariant feature learning framework. Mesh, point cloud, and multi-view image features are extracted by MeshNet, DGCNN, ResNet, and corresponding projection heads, respectively. With contrastive learning to minimum the feature similarity of positive pairs and maximum the feature similarity of negative pairs under modality- and view-invariant constraints, the modal- and view-invariant features can be learned with the proposed heterogeneous framework in the same universal space.

proposed self-supervised learning schema, two types of feature learning are formulated as supervision signals for contrastive learning to optimize the networks: modal-invariant feature learning and view-invariant feature learning.

Modal-invariant Feature Learning: The object identity information of 3D objects is utilized as the modality-invariant constraint to sample training pairs from different modalities. In this paper, the invariance from three pairs of different data modalities are constructed as training samples including: mesh-point (mesh and point cloud), mesh-image (mesh and image), and point-image (point cloud and image). Taking the mesh and point cloud pair as an example, in a training minibatch of k samples, a batch of k mesh features $\{f_m^{(1)}, \dots, f_m^{(k)}\}$ and k corresponding point cloud features $\{f_p^{(1)}, \dots, f_p^{(k)}\}$ are considered as the anchor and positive feature batches alternately with each other. Then, following the equations 1, 3, and 4, the complete cross-modal contrastive loss for the mesh and point cloud pair is indicated as L_{MP} . The cross-modal contrastive loss for the other two cross-modality pairs (mesh-image and point-image) are calculated in the same way indicated as L_{MI} and L_{PI} , respectively.

View-invariant Feature Learning: In image modality, two randomly selected views for each object are used for view-invariant contrastive learning as shown in Fig. 2. With the same loss functions 1, 3, and 4, the cross-view contrastive loss L_{II} is calculated with each image feature with $\{f_{i1}^{(1)}, \dots, f_{i1}^{(k)}\}$ and $\{f_{i2}^{(1)}, \dots, f_{i2}^{(k)}\}$ in the training minibatch.

When jointly trained with the two constraints, a linear

Algorithm 1 The proposed self-supervised feature learning algorithm by contrastive learning cross multimodality and multiviews.

```

minibatch size:  $k$ ; 2D image features:  $f_i$ ; 3D point cloud features:  $f_p$ ; 3D mesh
features:  $f_m$ ;
for all sampled mini-batch  $\{X^{(i)}\}_{i=1}^k$  do
  # feature extraction
  for all  $i \in \{1, \dots, k\}$  do
     $f_m^{(i)} = F_{m,h}(F_m(m^{(i)}))$ ;  $f_p^{(i)} = F_{p,h}(F_p(p^{(i)}))$ ;
     $f_{i1}^{(i)} = F_{img,h}(F_{img}(img_1^{(i)}))$ ;  $f_{i2}^{(i)} = F_{img,h}(F_{img}(img_2^{(i)}))$ ;
  end for
  # loss calculation under modality-invariant constraint
   $L_{MP} = l_{mp} + l_{pm}$ 
   $L_{MI} = l_{mi} + l_{im}$ 
   $L_{PI} = l_{pi} + l_{ip}$ 
  # loss calculation under view-invariant constraint
   $L_{II} = l_{i1i2} + l_{i2i1}$ 
  # final loss
   $\mathcal{L} = L_{MP} + L_{MI} + L_{PI} + L_{II}$ 
  update networks  $F_{img}$ ,  $F_{img,h}$ ,  $F_p$ ,  $F_{p,h}$ ,  $F_m$ , and  $F_{m,h}$  to minimize  $\mathcal{L}$ 
end for
return pre-trained networks  $F_{img}$ ,  $F_p$ , and  $F_m$ 

```

weighted combination of all loss functions is employed to optimize all the networks. The final loss to optimize the framework is as:

$$\mathcal{L} = L_{MP} + L_{MI} + L_{PI} + L_{II}. \quad (5)$$

The details of the joint training process are illustrated in Algorithm 1. After the jointly training finished, three networks F_{img} , F_p , and F_m are obtained as pre-trained models for three different modalities. The joint training enables the three feature extractors to map the features from different modalities and views into the same universal space.

3.2. Framework Architecture

As shown in Fig. 2, the MeshNet [9], dynamic graph convolutional neural network (DGCNN) [50], and ResNet [18] are employed as backbone networks to extract representation features from mesh, point cloud, and rendered images, respectively. $F_{m,h}$, $F_{p,h}$, $F_{img,h}$ are three corresponding two-layer fully connected projection heads to map the extracted representation features into an universe space for contrastive learning. The architecture of backbone networks is described as follows.

MeshNet: The backbone architecture for mesh data is MeshNet, denoted as F_m . MeshNet contains three main blocks: spatial descriptor, structural descriptor, and mesh convolution block. The spatial descriptor applies fully-connected layers (64, 64) to extract spatial features from faces center. The structural descriptor contains a face rotate convolution within fully-connected layers (32, 32) and (64, 64), and a face kernel correlation with 64 kernels. Two mesh convolution blocks are used to aggregate features with neighboring information which the input/output channels of spatial and structural features are configured as (64, 131, 256, 256) and (256, 256, 512, 512), respectively. After the two mesh convolution blocks, a fully-connected layer (1024) further fuses the neighboring features and a max-pooling layer is employed to extract 512-dimension global features from the aggregated features.

DGCNN: The 3D point cloud feature learning network (F_p) employs DGCNN as the backbone model due to its capability to model local structures of each point by dynamically constructed graphs. There are four EdgeConv layers and the number of kernels in each layer is 64, 64, 64, and 128, and the EdgeConv layers aim to construct graphs over k nearest neighbors calculated by KNN and the features for each point are calculated by an MLP over all the k closest points. After the four EdgeConv blocks, a 512-dimension fully connected layer is used to extract per-point features for each point and then a max-pooling layer is employed to extract global features for each object.

ResNet: ResNet18 is employed as the image feature capture network (F_{img}) for 2D images. It contains four convolution blocks with a number of {64, 128, 256, and 512} kernels. Each convolution block includes two convolution layers followed by a batch-normalization layer and a ReLU layer, except the first convolution block which consists of one convolution layer, one batch-normalization layer, and one max-pooling layer. A global average pooling layer, after the fourth convolution blocks, is used to obtain the global features for each image. Unless specifically pointed out, a 512-dimensional vector after the global average pooling layer is used for all our experiments.

4. Experimental Results

4.1. Experimental Setup

Self-supervised learning: The proposed framework is jointly trained on ModelNet40 dataset using a SGD optimizer with an initial learning rate of 0.001, the moment of 0.9, and weight decay of 0.0005. The network is optimized with a mini-batch size of 96 for 160,000 iterations and the learning rate decrease by 90% every 40,000 iteration. Data augmentation used for point cloud network includes randomly rotated between $[0, 2\pi]$ degrees along the up-axis, randomly jittered the position of each point by Gaussian noise with zero mean and 0.02 standard deviation. Data augmentation for images include randomly cropped and randomly flipped with 50% probability. Data augmentation for mesh includes random rotation with a degree between $[0, 2\pi]$.

Datasets: Two 3D object benchmarks: ModelNet40 [52] and ShapeNet [5] are used to evaluate the proposed method. The ModelNet40 dataset contains about 12.3k meshed models covering 40 object classes, while about 9.8k are used for training and about 2.5k for testing. The ShapeNet dataset contains 16 object categories with about 12.1k models for training and about 2.9k for testing.

Training data generation: The point cloud data and multi-view image data are sampled and rendered from same 3D mesh objects, respectively. Specifically, following [37], the point cloud set is sampled from surfaces of mesh objects by Farthest Point Sampling (FPS) algorithm. For each object, uniform 2,048 points are sampled and normalized into a unit sphere to keep the object shape as much as possible. Same as in [22], we employ Phong reflection model [36] as the rendering engine to render images from 180 virtual cameras (viewpoints) to capture perspective of mesh objects as comprehensive as possible. All virtual cameras are randomly placed along a sphere surface pointing toward the centroid of mesh objects, and one image is rendered from each camera. Note that two of the rendered images are randomly selected for each input training sample.

Evaluation of learned 2D and 3D features: The effectiveness of the self-supervised pre-trained backbone networks F_{img} , F_p , and F_m are validated on different downstream tasks for 3D objects including object recognition, few-shot recognition, part segmentation, in-domain and cross-modal retrieval. The features, from the universal space, extracted by the three backbones and corresponding projection heads ($F_{img,h}$, $F_{p,h}$, $F_{m,h}$) are used for the cross-modal retrieval task.

4.2. Transfer to Object Recognition Tasks

The proposed framework can jointly learn features for data with different modalities and views. We validate the effectiveness of the self-supervised pre-trained F_{img} , F_p , and

F_m on three down-stream supervised tasks: image recognition, point cloud object recognition, and mesh object recognition on the ModelNet40 dataset. Specifically, three linear SVM classifiers are trained based on the extracted features by F_{img} , F_p , and F_m , respectively. The performance of the SVMS on the testing splits of ModelNet40 dataset are reported and compared. Each feature for the 2D classifier is average from v extracted features of v random views.

Table 1. The performance of object recognition tasks by using self-supervised learned models as feature extractors on the ModelNet40 dataset. "Views" indicates how many views of images are used to obtain the image features.

Network	Modality	Views	Accuracy (%)
F_{img}	Image	1	78.0
F_{img}	Image	2	83.1
F_{img}	Image	4	85.8
F_{img}	Image	8	87.2
F_{img}	Image	12	87.7
F_{img}	Image	36	88.2
F_p	Point Cloud	–	89.3
F_m	Mesh	–	87.7

As shown in Table 1, the self-supervised pre-trained networks F_{img} , F_p , and F_m obtain high accuracy (almost 90%) on object recognition tasks with different modalities, showing that the discriminative semantic features are indeed learned through the self-supervised learning process. For the image network, when only one view is available, the performance is only 78%, and the performance is significantly boosted when more views are available. Given enough image views, the three networks for the three modalities obtained comparable performance showing that the proposed framework learn robust features for all the modalities.

4.3. Transfer to Few-shot Object Recognition Task

To further evaluate the generalization ability of the learned features, we also evaluate the self-supervised pre-trained F_{img} , F_p , and F_m on 2D/3D few-shot object recognition tasks and showing the performance in Table 2 on ModelNet40 dataset. Similar to the settings in Section 4.2, three corresponding linear SVM classifiers are trained based on the features of 5, 10, and 20 labeled data for each object category, and the image features for 2D recognition task are generated by max-pooling.

As shown in Table 2, even only a few labeled data are available for each class, the networks on mesh and point cloud obtain relative high performance for few-shot learning. When only one view of images available, the performance for object recognition with images are much lower than the other two modalities. The performance of object recognition with images is significantly boosted up when more views are available. Overall, the features from mesh

Table 2. The performance of few-shot object recognition tasks of the features learned by the proposed self-supervised learning method on ModelNet40 dataset. "S-#" indicates the number of shots for each class.

Network	Input	Views	S-5 Acc	S-10 Acc	S-20 Acc
F_{img}	Image	1	64.0	65.9	70.2
F_{img}	Image	2	66.0	70.7	75.6
F_{img}	Image	4	66.0	74.2	77.6
F_{img}	Image	8	68.4	73.9	78.8
F_{img}	Image	12	70.4	74.6	79.1
F_p	Point Cloud	–	66.1	71.8	77.8
F_m	Mesh	–	67.9	73.3	79.0

modality are more robust than the other two modalities.

4.4. Transfer to 3D Part Segmentation Task

For a more thorough effectiveness validation of the learned features across different tasks, we further conduct transfer learning experiments on 3D part segmentation task on the ShapeNet point cloud dataset with a few labeled data available. Since this data only contains labels for the point cloud data, only F_p is evaluated on part segmentation task. Four fully connected layers are added on the top of F_p , and the outputs from all the four EdgeConv blocks and the global features are used to predict the pixel-wise labels. We vary the amount of training data on three experimental setups: (1) with random initialization and supervised training from scratch by the same network [37], (2) updating parameters on four newly added layers with frozen F_p , and (3) fine-tuning parameters with the pre-trained F_p (unfrozen). The performance is shown in Table 3.

Table 3. The performance of the three types of settings on different amount of training data from the ShapeNet dataset for object part segmentation task.

Network	Training data	Overall Acc	Class mIOU	Instance mIOU
Scratch [37]	1%	84.4%	54.1%	68.0%
F_p -Frozen	1%	86.2%	58.1%	70.9%
F_p -Unfrozen	1%	88.0%	60.1%	73.1%
Scratch [37]	2%	86.6%	62.7%	71.9%
F_p -Frozen	2%	88.0%	60.6%	73.4%
F_p -Unfrozen	2%	89.5%	66.7%	76.2%
Scratch [37]	5%	88.5%	63.1%	75.1%
F_p -Frozen	5%	89.5%	65.1%	76.0%
F_p -Unfrozen	5%	91.0%	69.6%	78.7%

As shown in Table 3, for both F_p -Frozen and F_p -Unfrozen, the performance of 3D part segmentation can

be boosted up in overall accuracy, class mean IOU, and instance mean IOU. Specifically, when only 1% labeled data available, the parameter-frozen setup can significantly (+4% on class mIOU, and +2.9% on instance mIOU) and increases the performance than training from scratch. It validates that F_p is able to learn semantic features from modality-invariant constraints and transfer them across datasets and tasks. As more data are available for training, the overall performance of the network keeps improving and the network significantly benefits from the learned weights. These results suggest that the proposed pretext task lead to learn strong features that are able to be generalized to other tasks.

4.5. Transfer to Retrieval and Cross-modal Retrieval Tasks

Compared to all other self-supervised learning models for 3D objects, our method learns modal- and view-invariant features which makes the features of different data modalities be directly comparable. To evaluate the quality of the modal- and view-invariant features, we propose to evaluate them on in-domain and cross-domain retrieval tasks. The performance on the cross-domain retrieval task can show generalizability of the modal-invariance while the performance on the in-domain retrieval task can show generalizability of view-invariance of the learned features. The features for different modalities are extracted by the self-supervised pre-trained backbone networks ($F_{img,h}$, $F_{p,h}$, $F_{m,h}$), and then followed by **L1** normalization. The Euclidean distance of features is employed to indicate the similarity of two features. All the experiments for in-domain retrieval and cross-domain retrieval tasks are performed on ModelNet40 dataset.

Table 4. Performance of in-domain retrieval tasks with the learned mesh, point cloud, and image features on ModelNet40 dataset. Results of XMV [22] are reproduced. The networks with * are pre-trained on ImageNet dataset.

Network	Source	Views	mAP
$F_m + F_{m,h}$	Mesh	—	62.4
XMV [22]	Point Cloud	—	48.4
$F_p + F_{p,h}$	Point Cloud	—	62.1
ResNet18 [18]*	Image	1	27.3
XMV [22]	Image	1	30.3
$F_{img} + F_{img,h}$	Image	1	57.9
ResNet18 [18]*	Image	2	34.6
XMV [22]	Image	2	36.3
$F_{img} + F_{img,h}$	Image	2	60.5
ResNet18 [18]*	Image	4	41.6
XMV [22]	Image	4	46.3
$F_{img} + F_{img,h}$	Image	4	62.3

In-domain Retrieval: The performance of three retrieval tasks (image-to-image, point-to-point, and mesh-to-

mesh) are shown in Table 4. For a fair comparison, the networks used in each domain are with the same architecture and trained on the same dataset, except ResNet18 [18] which is pre-trained on ImageNet dataset. The results from XMV [22] are tested by the released pre-trained model. For all the in-domain retrieval tasks, our network achieves relatively high performance and significantly outperforms the recent state-of-the-art self-supervised learning models and the ImageNet pre-trained model. Even when only 1 image view for each object is available, our model achieves 57.9% mAP for the in-domain retrieval showing that our model indeed learns view-invariant features. When 4 views of images for each object is available, the performance of in-domain retrieval task improves by 4.4% on ModelNet40 dataset.

Table 5. Performance of **cross-modal** retrieval tasks with the learned images, point cloud, and mesh features on ModelNet40 dataset.

Source	Target	Views	mAP
Mesh	Point Cloud	—	61.6
Mesh	Image	1	58.9
Mesh	Image	2	60.8
Mesh	Image	4	61.7
Point Cloud	Mesh	—	62.0
Point Cloud	Image	1	59.0
Point Cloud	Image	2	60.8
Point Cloud	Image	4	61.7
Image	Point Cloud	1	59.5
Image	Point Cloud	2	60.7
Image	Point Cloud	4	61.7
Image	Mesh	1	59.8
Image	Mesh	2	61.0
Image	Mesh	4	61.7

Cross-modal retrieval: The jointly learned modal-invariant features in the universal feature space for three different data modalities make the cross-modal retrieval for 3D objects possible, which is, as far as we know, not explored by any other self-supervised or supervised methods. The cross-modal retrieval task aims to match input data from one modality to different representations from another modality. Here as shown in the Table 5, the feature representation abilities for different modalities are extensively evaluated by six cross-modal retrieval tasks (image-to-point, point-to-image, image-to-mesh, mesh-to-image, mesh-to-point, and point-to-mesh). Our models achieve relatively high performance on all the six different cross-modal combinations showing that the network indeed learns the modal-invariant features. In general, the retrieval accuracy between mesh and point cloud modalities is better than image-involved retrieval due to the inputs of mesh and point cloud contain

Table 6. The comparison with 2D state-of-the-art methods for multi-view 3D object recognition on ModelNet40 dataset.

Network	Supervised	#views	Acc (%)
MVCNN [45]	Yes	1	85.1
DeCAF [8]	Yes	1	83.0
Fisher Vector [39]	No	1	78.8
XMV [22]	No	1	72.5
F_{img} (Ours)	No	1	78.0
DeCAF [8]	Yes	12	88.6
MVCNN [45]	Yes	12	88.6
XMV [22]	No	12	87.3
F_{img} (Ours)	No	12	87.7

overall structure information of 3D objects, while a few input views (one or two) are insufficient. When more views (four) are available, the image-involved retrieval accuracy is basically the same. The qualitative visualization results of the top-10 ranking lists for six query samples on ModelNet40 dataset are shown in Fig. 3. Only one view for each object is used as query or galleries. For objects with unique structures like the airplane, guitar, and car, our models achieves high precision for these classes.

4.6. Comparison with the State-of-the-art Methods

Object recognition with 2D multi-view images. The performance of our self-supervised pre-trained F_{img} and the state-of-the-art image-based methods on the ModelNet40 benchmark is shown in Table 6. Methods with multi-view inputs are compared, including hand-crafted model [39] and supervised feature learning models [8, 45, 22]. The setups of our models are same as in subsection 4.2. Note that DeCAF [8] and MVCNN [45] demand large-scale labeled data ImageNet1K for pre-training. XMV [22] is pre-trained with two types of modalities (image and point cloud), and the learned features are not modality-invariant. When using same number of views, the performance of our model F_{img} consistently outperforms the state-of-the-art self-supervised learning method [22] and obtained comparable performance with the supervised methods [8, 45].

3D object recognition with point cloud and mesh. Table 7 compares the proposed self-supervised pre-trained models F_p and F_m against both self-supervised learning methods [1, 6, 10, 12, 16, 22, 25, 42, 51, 54, 57] and supervised learning methods [9, 10, 21, 26, 29, 38, 43, 49, 50] on the ModelNet40 benchmark. Our self-supervised learning approach achieves comparable performance to the supervised methods on the ModelNet40 dataset. The performance of our model are very close (0.5% lower) to previous self-supervised learning methods, while the learned modal-invariant features are applicable for more downstream tasks such as retrieval task. Worth to note that most of the self-

Table 7. The comparison with the state-of-the-art methods for 3D point cloud object recognition on ModelNet40 dataset. * indicates the results in based on mesh modality.

Unsupervised		Supervised	
SPH [25]	68.2	PointCNN [21]	86.1
T-L Network [12]	74.4	PointNet [29]	89.2
LFD [6]	75.5	PointNet++ [38]	90.7
VConv-DAE [42]	75.5	KCNet [43]	91.0
3D-GAN [51]	83.3	SpecGCN [49]	91.5
Latent-GAN [1]	85.7	MRTNet [10]	91.7
MRTNet-VAE [10]	86.4	KDNet [26]	91.8
Contrast [55]	86.8	MeshNet* [9]	91.9
FoldingNet [54]	88.4	DGCNN [50]	92.2
PointCapsNet [57]	88.9		
MultiTask [16]	89.1		
XMV [22]	89.8		
F_m * (Ours)	87.7		
F_p (Ours)	89.3		

supervised learning only learn features for point cloud data, while our method is able to learn modal- and view-invariant features for different modalities, and it can be easily extend to other modalities.

5. Conclusion

In this paper, we have proposed a novel self-supervised learning method to jointly learn features which are invariant to different modalities and views. Different from all the previous self-supervised learning methods, our method is able to learn features for different modalities in the same universal space which makes it possible to explore a new task, i.e., cross-modal 3D object retrieval. The image features, mesh features, and point cloud features learned by three different networks have been extensively tested on different tasks including 3D object recognition, few-shot learning, part segmentation, 3D objects retrieval and cross-modal retrieval, and demonstrated the strong generalizability of the learned features.

6. Acknowledgement

This material is partially based upon the work supported by National Science Foundation (NSF) under award number IIS-1400802.

References

- [1] Panos Achlioptas, Olga Diamanti, Ioannis Mitliagkas, and Leonidas Guibas. Learning representations and generative models for 3d point clouds. *arXiv preprint arXiv:1707.02392*, 2017. 1, 2, 8

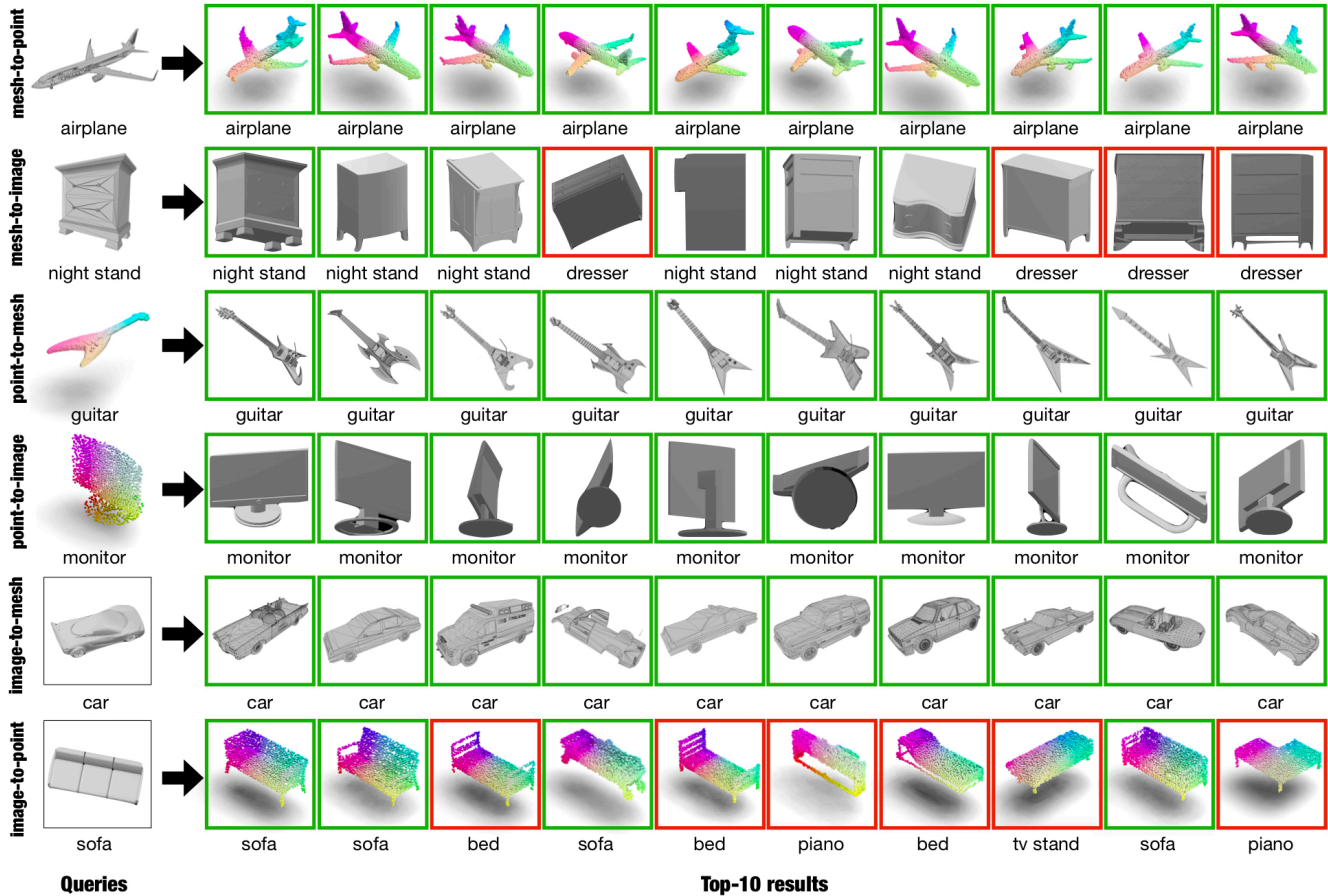


Figure 3. Top-10 ranking lists for six query samples on ModelNet40 dataset by our models. The results with green boundaries belong to the same category as the query, and images with red borders do not.

- [2] Yuki Markus Asano, Christian Rupprecht, and Andrea Vedaldi. Self-labelling via simultaneous clustering and representation learning. *arXiv preprint arXiv:1911.05371*, 2019. 1
- [3] Philip Bachman, R Devon Hjelm, and William Buchwalter. Learning representations by maximizing mutual information across views. In *Advances in Neural Information Processing Systems*, pages 15509–15519, 2019. 2, 3
- [4] Mathilde Caron, Piotr Bojanowski, Armand Joulin, and Matthijs Douze. Deep clustering for unsupervised learning of visual features. In *ECCV*, 2018. 2
- [5] Angel X Chang, Thomas Funkhouser, Leonidas Guibas, Pat Hanrahan, Qixing Huang, Zimo Li, Silvio Savarese, Manolis Savva, Shuran Song, Hao Su, et al. Shapenet: An information-rich 3d model repository. *arXiv preprint arXiv:1512.03012*, 2015. 5
- [6] Ding-Yun Chen, Xiao-Pei Tian, Yu-Te Shen, and Ming Ouhyoung. On visual similarity based 3d model retrieval. In *Computer graphics forum*, pages 223–232. Wiley Online Library, 2003. 8
- [7] Ting Chen, Simon Kornblith, Mohammad Norouzi, and Geoffrey Hinton. A simple framework for contrastive learning of visual representations. *arXiv preprint arXiv:2002.05709*, 2020. 1, 2, 3
- [8] Jeff Donahue, Yangqing Jia, Oriol Vinyals, Judy Hoffman, Ning Zhang, Eric Tzeng, and Trevor Darrell. Decaf: A deep convolutional activation feature for generic visual recognition. In *International conference on machine learning*, pages 647–655, 2014. 8
- [9] Yutong Feng, Yifan Feng, Haoxuan You, Xibin Zhao, and Yue Gao. Meshnet: mesh neural network for 3d shape representation. In *Proceedings of the AAAI Conference on Artificial Intelligence*, volume 33, pages 8279–8286, 2019. 5, 8
- [10] Matheus Gadelha, Rui Wang, and Subhransu Maji. Multiresolution tree networks for 3d point cloud processing. In *Proceedings of the European Conference on Computer Vision (ECCV)*, pages 103–118, 2018. 1, 2, 8
- [11] Spyros Gidaris, Praveer Singh, and Nikos Komodakis. Unsupervised representation learning by predicting image rotations. In *ICLR*, 2018. 2
- [12] Rohit Girdhar, David F Fouhey, Mikel Rodriguez, and Abhinav Gupta. Learning a predictable and generative vector representation for objects. In *European Conference on Computer Vision*, pages 484–499. Springer, 2016. 8

- [13] Ian Goodfellow, Jean Pouget-Abadie, Mehdi Mirza, Bing Xu, David Warde-Farley, Sherjil Ozair, Aaron Courville, and Yoshua Bengio. Generative adversarial nets. In *NIPS*, pages 2672–2680, 2014. 2
- [14] Daniel Gordon, Kiana Ehsani, Dieter Fox, and Ali Farhadi. Watching the world go by: Representation learning from unlabeled videos. *arXiv preprint arXiv:2003.07990*, 2020. 2, 3
- [15] Michael Gutmann and Aapo Hyvärinen. Noise-contrastive estimation: A new estimation principle for unnormalized statistical models. In *Proceedings of the Thirteenth International Conference on Artificial Intelligence and Statistics*, pages 297–304, 2010. 2
- [16] Kaveh Hassani and Mike Haley. Unsupervised multi-task feature learning on point clouds. In *Proceedings of the IEEE International Conference on Computer Vision*, pages 8160–8171, 2019. 1, 2, 8
- [17] Kaiming He, Haoqi Fan, Yuxin Wu, Saining Xie, and Ross Girshick. Momentum contrast for unsupervised visual representation learning. *arXiv preprint arXiv:1911.05722*, 2019. 1, 2, 3
- [18] Kaiming He, Xiangyu Zhang, Shaoqing Ren, and Jian Sun. Deep residual learning for image recognition. In *Proceedings of the IEEE conference on computer vision and pattern recognition*, pages 770–778, 2016. 5, 7
- [19] Olivier J Hénaff, Ali Razavi, Carl Doersch, SM Eslami, and Aaron van den Oord. Data-efficient image recognition with contrastive predictive coding. *arXiv preprint arXiv:1905.09272*, 2019. 3
- [20] R Devon Hjelm, Alex Fedorov, Samuel Lavoie-Marchildon, Karan Grewal, Phil Bachman, Adam Trischler, and Yoshua Bengio. Learning deep representations by mutual information estimation and maximization. *arXiv preprint arXiv:1808.06670*, 2018. 3
- [21] Binh-Son Hua, Minh-Khoi Tran, and Sai-Kit Yeung. Point-wise convolutional neural networks. In *Proceedings of the IEEE Conference on Computer Vision and Pattern Recognition*, pages 984–993, 2018. 8
- [22] Longlong Jing, Yucheng Chen, Ling Zhang, Mingyi He, and Yingli Tian. Self-supervised feature learning by cross-modality and cross-view correspondences. *arXiv preprint arXiv:2004.05749*, 2020. 1, 2, 5, 7, 8
- [23] Longlong Jing and Yingli Tian. Self-supervised spatiotemporal feature learning by video geometric transformations. *arXiv preprint arXiv:1811.11387*, 2(7):8, 2018. 2
- [24] Longlong Jing and Yingli Tian. Self-supervised visual feature learning with deep neural networks: A survey. *arXiv preprint arXiv:1902.06162*, 2019. 1
- [25] Michael Kazhdan, Thomas Funkhouser, and Szymon Rusinkiewicz. Rotation invariant spherical harmonic representation of 3 d shape descriptors. In *Symposium on geometry processing*, volume 6, pages 156–164, 2003. 8
- [26] Roman Klokov and Victor Lempitsky. Escape from cells: Deep kd-networks for the recognition of 3d point cloud models. In *Proceedings of the IEEE International Conference on Computer Vision*, pages 863–872, 2017. 8
- [27] Bruno Korbar, Du Tran, and Lorenzo Torresani. Cooperative learning of audio and video models from self-supervised synchronization. In *NIPS*, pages 7773–7784, 2018. 2
- [28] Christian Ledig, Lucas Theis, Ferenc Huszar, Jose Caballero, Andrew Cunningham, Alejandro Acosta, Andrew P. Aitken, Alykhan Tejani, Johannes Totz, Zehan Wang, and Wenzhe Shi. Photo-realistic single image super-resolution using a generative adversarial network. In *CVPR*, 2017. 2
- [29] Chun-Liang Li, Manzil Zaheer, Yang Zhang, Barnabas Poczos, and Ruslan Salakhutdinov. Point cloud gan. *arXiv preprint arXiv:1810.05795*, 2018. 1, 2, 8
- [30] Ishan Misra and Laurens van der Maaten. Self-supervised learning of pretext-invariant representations. *arXiv preprint arXiv:1912.01991*, 2019. 1, 3
- [31] Ishan Misra, C Lawrence Zitnick, and Martial Hebert. Shuffle and learn: unsupervised learning using temporal order verification. In *ECCV*, pages 527–544. Springer, 2016. 2
- [32] Mehdi Noroozi and Paolo Favaro. Unsupervised learning of visual representations by solving jigsaw puzzles. In *ECCV*, 2016. 2
- [33] Aaron van den Oord, Yazhe Li, and Oriol Vinyals. Representation learning with contrastive predictive coding. *arXiv preprint arXiv:1807.03748*, 2018. 3
- [34] Deepak Pathak, Ross Girshick, Piotr Dollár, Trevor Darrell, and Bharath Hariharan. Learning features by watching objects move. In *CVPR*, volume 2, 2017. 2
- [35] Mandela Patrick, Yuki M Asano, Ruth Fong, João F Henriques, Geoffrey Zweig, and Andrea Vedaldi. Multi-modal self-supervision from generalized data transformations. *arXiv preprint arXiv:2003.04298*, 2020. 3
- [36] Bui Tuong Phong. Illumination for computer generated pictures. *Communications of the ACM*, 18(6):311–317, 1975. 5
- [37] Charles R Qi, Hao Su, Kaichun Mo, and Leonidas J Guibas. Pointnet: Deep learning on point sets for 3d classification and segmentation. In *Proceedings of the IEEE conference on computer vision and pattern recognition*, pages 652–660, 2017. 5, 6
- [38] Charles Ruizhongtai Qi, Li Yi, Hao Su, and Leonidas J Guibas. Pointnet++: Deep hierarchical feature learning on point sets in a metric space. In *Advances in neural information processing systems*, pages 5099–5108, 2017. 8
- [39] Jorge Sánchez, Florent Perronnin, Thomas Mensink, and Jakob Verbeek. Image classification with the fisher vector: Theory and practice. *International journal of computer vision*, 105(3):222–245, 2013. 8
- [40] Jonathan Sauder and Bjarne Sievers. Self-supervised deep learning on point clouds by reconstructing space. In *Advances in Neural Information Processing Systems*, pages 12942–12952, 2019. 2
- [41] Florian Schroff, Dmitry Kalenichenko, and James Philbin. Facenet: A unified embedding for face recognition and clustering. In *Proceedings of the IEEE conference on computer vision and pattern recognition*, pages 815–823, 2015. 2, 3
- [42] Abhishek Sharma, Oliver Grau, and Mario Fritz. Vconv-dae: Deep volumetric shape learning without object labels. In *European Conference on Computer Vision*, pages 236–250. Springer, 2016. 8

- [43] Yiru Shen, Chen Feng, Yaoqing Yang, and Dong Tian. Mining point cloud local structures by kernel correlation and graph pooling. In *Proceedings of the IEEE conference on computer vision and pattern recognition*, pages 4548–4557, 2018. 8
- [44] Nitish Srivastava, Elman Mansimov, and Ruslan Salakhutdinov. Unsupervised Learning of Video Representations using LSTMs. In *ICML*, 2015. 2
- [45] Hang Su, Subhransu Maji, Evangelos Kalogerakis, and Erik Learned-Miller. Multi-view convolutional neural networks for 3d shape recognition. In *Proceedings of the IEEE international conference on computer vision*, pages 945–953, 2015. 8
- [46] Yongbin Sun, Yue Wang, Ziwei Liu, Joshua E Siegel, and Sanjay E Sarma. Pointgrow: Autoregressively learned point cloud generation with self-attention. *arXiv preprint arXiv:1810.05591*, 2018. 1, 2
- [47] Ali Thabet, Humam Alwassel, and Bernard Ghanem. Mortonnet: Self-supervised learning of local features in 3d point clouds. *arXiv preprint arXiv:1904.00230*, 2019. 2
- [48] Yonglong Tian, Dilip Krishnan, and Phillip Isola. Contrastive multiview coding. *arXiv preprint arXiv:1906.05849*, 2019. 3
- [49] Chu Wang, Babak Samari, and Kaleem Siddiqi. Local spectral graph convolution for point set feature learning. In *Proceedings of the European conference on computer vision (ECCV)*, pages 52–66, 2018. 8
- [50] Yue Wang, Yongbin Sun, Ziwei Liu, Sanjay E Sarma, Michael M Bronstein, and Justin M Solomon. Dynamic graph cnn for learning on point clouds. *ACM Transactions on Graphics (TOG)*, 38(5):1–12, 2019. 5, 8
- [51] Jiajun Wu, Chengkai Zhang, Tianfan Xue, Bill Freeman, and Josh Tenenbaum. Learning a probabilistic latent space of object shapes via 3d generative-adversarial modeling. In *Advances in neural information processing systems*, pages 82–90, 2016. 1, 2, 8
- [52] Zhirong Wu, Shuran Song, Aditya Khosla, Fisher Yu, Linguang Zhang, Xiaoou Tang, and Jianxiong Xiao. 3d shapenets: A deep representation for volumetric shapes. In *Proceedings of the IEEE conference on computer vision and pattern recognition*, pages 1912–1920, 2015. 5
- [53] Zhirong Wu, Yuanjun Xiong, Stella X Yu, and Dahua Lin. Unsupervised feature learning via non-parametric instance discrimination. In *Proceedings of the IEEE Conference on Computer Vision and Pattern Recognition*, pages 3733–3742, 2018. 3
- [54] Yaoqing Yang, Chen Feng, Yiru Shen, and Dong Tian. Foldingnet: Point cloud auto-encoder via deep grid deformation. In *Proceedings of the IEEE Conference on Computer Vision and Pattern Recognition*, pages 206–215, 2018. 1, 2, 8
- [55] Ling Zhang and Zhigang Zhu. Unsupervised feature learning for point cloud understanding by contrasting and clustering using graph convolutional neural networks. In *2019 International Conference on 3D Vision (3DV)*, pages 395–404. IEEE, 2019. 1, 2, 8
- [56] Richard Zhang, Phillip Isola, and Alexei A Efros. Colorful image colorization. In *ECCV*, pages 649–666. Springer, 2016. 2
- [57] Yongheng Zhao, Tolga Birdal, Haowen Deng, and Federico Tombari. 3d point capsule networks. In *Proceedings of the IEEE Conference on Computer Vision and Pattern Recognition*, pages 1009–1018, 2019. 1, 2, 8